Lunar and J2 perturbations of the metric associated to the averaged orbital transfer

Bernard Bonnard, Helen Henninger, Jérémy Rouot

Lunar and J2 perturbations of the metric associated to the averaged orbital transfer

Bernard Bonnard, Helen Henninger and Jérémy Rouot

Dedicated to Hélène Frankowska and Héctor Sussmann

Abstract. In a series of previous article [1,2], we introduced a Riemannian metric associated to the energy minimizing orbital transfer with low propulsion. The aim of this article is to study the deformation of this metric due to the standard perturbations in space mechanics, e.g. oblate spheroid shape of the Earth and lunar attraction. Using Hamiltonian formalism, we describe the effects of the perturbations on the orbital transfers and the deformation of the conjugate and cut loci of the original metric.

1. Introduction

Recent space missions like lunar Smart-1 mission, Boeing orbital transfer, using electric propulsion are innovative design feature to reduce launch costs and lead to the analyse of the low thrust controlled Kepler equation using averaging techniques in optimal control. Pioneering work in this direction associated to the energy minimization problem are due to Edelbaum [7, 8], Epenoy-Geffroy [9, 10] and more recently to Bonnard-Caillau [1, 2]. Under some simplifying assumption they lead to the definition of a Riemannian distance between Keplerian orbits, and this is a preliminary step in computing the time minimal or find mass maximizing solutions using numerical continuation techniques [5].

The objective of this article is to analyse the deformation of this metric taking into account the oblate ellipsoid of revolution shape of the Earth (the J_2-effect) and the lunar perturbation both of which affect a wide range of missions. Again in the framework of the continuation techniques, we shall

Work supported in part by the French Space Agency CNES, R&T action R-S13/BS-005-012 and by the region Provence-Alpes-Côte d'Azur.

make simplifying assumptions. The main point is to deduce from the averaged system the qualitative policy to make the transfer and to initialize the shooting algorithm.

Making such assumptions leads to the analysis of a Zermelo navigation problem defined by an Hamiltonian which is a deformation of the Hamiltonian associated to the Riemannian metric and complete analysis of the transfer is made using continuation about trajectories computations and conjugate and cut analysis.

The organization of this article is the following. In section 2, we recall the computations and properties of the Riemannian metric based on [1]. In section 3, we present the J_2 and lunar perturbation and we describe the averaged system. In section 4, we give numerical simulations computations on extremal trajectories and on conjugate loci.

2. The Riemannian metric

The controlled Kepler equation, assuming the mass constant can be normalized to

$$\frac{d^2q}{dt^2} = -\frac{q}{|q|^3} + u \tag{1}$$

where $q = (q_1, q_2, q_3)$ is the position of the satellite and the thrust is bounded by $|u| \leq \epsilon$. The thrust can be decomposed in a moving frame $u = u_1F_1 + u_2F_2 + u_3F_3$ e.g. the so-called radial-orthoradial frame: $F_1 = \frac{q}{|q|}, F_2 = F_3 \wedge F_1$ and $F_3 = \frac{q \wedge \dot{q}}{|q \wedge \dot{q}|}$. The state of the system is described by an angle: the true longitude l and by five equinoctial elements x corresponding to first integrals of the uncontrolled motion. For instance, $x = (P, e, h)$ where P is the semi-latus rectum of the osculating cone, $e = (e_x, e_y)$ is the eccentricity vector and $h = (h_x, h_y)$ is the inclination vector. We restrict the system to the elliptic domain, that is to the manifold $\mathcal{X}$ of elliptic trajectories of the Kepler equation $\mathcal{X} = \{P > 0, |e| < 1\}$.

The system takes the form

$$\frac{dx}{dt} = \sum_{i=1}^{3} u_i F_i(x, l)$$
$$\frac{dl}{dt} = w_0(x, l) + g(x, l, u).$$

An important problem is to transfer the satellite between coplanar orbits, the corresponding subsystem is deduced by setting both the inclination h and the control u_3 to zero.

The energy minimization problem is studied in detail in [1] and we present only the main results.

The control is rescaled using $u = \epsilon v$, $|v| \leq 1$ to introduce the small parameter ϵ and we consider the energy minimization problem to transfer the system from (x_0, l_0) to a terminal orbit x_F. The terminal cumulated

longitude is also fixed to l_F. Parametrizing the trajectory by the cumulated longitude l, the system is written

$$\frac{dx}{dl} = \frac{\epsilon}{w_0(x,l) + \epsilon g(x,l,u)} \sum_{i=1}^{3} v_i F_i(x,l)$$

and the cost function to minimize is

$$\epsilon^2 \int_{l_0}^{l_F} \frac{|v|^2 dl}{w_0(x,l) + \epsilon g(x,l,u)}.$$

In order to perform the analytic computation, we first relax the bound $|v| \leq 1$. Indeed, for a fixed ϵ, the constraint will be fulfilled by a big enough final longitude l_F.

Using the maximum principle [14], optimal trajectories are extremals, integral curves of the following Hamiltonian

$$H_\epsilon(x,l,p,v) = \frac{\epsilon}{w_0(x,l) + \epsilon g(x,l,u)} (p^0 \epsilon |v|^2 + \sum_{i=1}^{3} v_i P_i)$$

where $p^0 \leq 0$ and $P_i = \langle p, F_i \rangle, i = 1,2,3$. In the normal case $p^0 < 0$ and it can be normalized to $-\frac{1}{2\epsilon}$. As a result, up to first order ϵ, we have the approximation

$$H_\epsilon(x,l,p,v) = \frac{\epsilon}{w_0(x,l)} \left(-\frac{1}{2}|v|^2 + \sum_{i=1}^{3} v_i P_i \right) + o(\epsilon).$$

In the computation of the averaged system, we can used the first order approximation

$$H(x,l,p,v) = \frac{1}{2} \sum_{i=1}^{3} \left(\frac{P_i}{\sqrt{w_0}} \right)^2.$$

Definition 2.1. The averaged Hamiltonian is

$$\overline{H}(x,p) = \frac{1}{2\pi} \int_0^{2\pi} H(x,l,p) dl.$$

Coplanar case. We have $H = \frac{1}{2}(P_1^2 + P_2^2)$ and the averaged system is expressed in the coordinates (n, ρ, θ) where n is the mean movement, ρ is the eccentricity and θ is the polar angle of the vector (e_x, e_y) (we also have $\rho = \sqrt{e_x^2 + e_y^2}$),

$$P = \frac{1-\rho^2}{n^{\frac{2}{3}}}, \ e_x = \rho cos(\theta), \ e_y = \rho sin(\theta),$$

and we have

Proposition 2.2. *In coordinates (n, ρ, θ), the averaged Hamiltonian is*

$$\overline{H_1} = \frac{1}{4n^{\frac{5}{3}}} \left[18n^2 p_n^2 + 5(1-\rho^2) p_\rho^2 + (5 - 4\rho^2) \frac{p_\theta^2}{\rho^2} \right]$$

and $\overline{H_1}$ *is the Hamiltonian of the Riemannian metric*

$$ds^2 = \frac{1}{9n^{\frac{1}{3}}}dn^2 + \frac{2n^{\frac{5}{3}}}{5(1-\rho^2)}d\rho^2 + \frac{2n^{\frac{5}{3}}}{5-4\rho^2}\rho^2 d\theta^2.$$

The coordinates (n, ρ, θ) *are orthogonal coordinates.*

Non Coplanar Case. The complete Hamiltonian is $H = \frac{1}{2}(P_1^2 + P_2^2 + P_3^2)$. As previously we use (n, ρ, θ) as coordinates and we make a polar representation of h,

$$h_x = \delta cos(\Omega), h_y = \delta sin(\Omega)$$

where the angle Ω is the longitude of the ascending node. Introducing $\omega = \theta - \Omega$, the angle of the pericenter, and denoting

$$p_{\theta\Omega} = \frac{2\delta^2}{\delta^2+1}p_\theta + p_\Omega,$$

we have

Proposition 2.3. *The averaged Hamiltonian of the non-coplanar transfer is*

$$\overline{H} = \overline{H_1} + \overline{H_2}$$

with

$$\overline{H_2} = \frac{(\delta^2+1)^2}{16n^{\frac{5}{3}}} \times \left[\frac{1+4\rho^2}{1-\rho^2}(cos(\omega)p_\delta + sin(\omega)\frac{p_{\theta\Omega}}{\delta})^2 + (-sin(\omega)p_\delta + cos(\omega)\frac{p_{\theta\Omega}}{\delta})^2\right]$$

and $\overline{H}$ *is associated with a five-dimensional Riemannian metric.*

The perturbed case. The system is written

$$\frac{dx}{dl} = P(x, l, l') + \sum_{i=1}^{3} u_i F_i(x, l)$$

where P is the perturbation superposing the J_2-effect and the lunar perturbation, depending on an additional angular variable l', e.g. the lunar longitude or the mean anomaly. The averaging procedure will produce an Hamiltonian which is the superposition of

- An averaged perturbation denoted $\overline{H_p}$.
- The averaged Hamiltonian $\overline{H}$ computed before and corresponding to the minimization problem.

  This leads to the definition of a Zermelo navigation problem [3, 4].

Definition 2.4. A Zermelo navigation problem on a n-dimensional Riemannian manifold $(\mathcal{X}, g)$ is a time minimal problem associated to the system

$$\frac{dx}{dl} = F_0(x) + \sum_{i=1}^{n} u_i F_i(x)$$

where F_i form an orthonormal frame for the metric g and $|u| \leq 1$. Observe that F_0 represents the current of magnitude $|F_0|_g$. If $|F_0|_g < 1$, this defines a Finsler metric.

Definition 2.5. If we apply the Maximum principle to the previous optimal problem this defines an Hamiltonian which is homogeneous in p. Conversely, one can associate to the Hamiltonian $H = \overline{H_p} + \lambda\sqrt{\overline{H}}$ a Zermelo navigation problem, where λ is a scaling parameter associated to the maximal control magnitude.

3. The perturbations

3.1. Preliminairies

First of all, the perturbations lead to the definition of a vector field whose trajectories behavior can be roughly classified in the framework of properties of conservative systems in the large, introduced for the three-body problem by Poincaré [13] and see [11] for a modern presentation.

Definition 3.1. Let V be a smooth complete vector field on a manifold $\mathcal{M}$ and let $x(t, x_0)$ be the solution starting at $t = 0$ from x_0. The point x_0 is called Poisson-stable if for every neighbourhood U of x_0 and every $T \geq 0$, there exists $t_1, t_2 \geq T$ such that $x(t_1, x_0)$ and $x(-t_2, x_0)$ belong to U. The point x_0 is said to be departing if for each compact set K there exists $T \geq 0$ such that if $|t| \geq T$, $x(t, x_0) \notin K$.

Theorem 3.2. *Let V be smooth complete conservative vector field on $(\mathcal{M}, \omega)$, then almost every point is Poisson-stable or departing.*

Coordinates. The satellite position and velocity are represented by $(q, \dot{q})$ and we denote (q, p) the standard symplectic coordinates. The motion of the satellite which is defined up to a proper normalization by Kepler Hamiltonian

$$H(q, p) = \frac{1}{2}|p|^2 - \frac{1}{|q|}.$$

To analyze the effect of a perturbing force deriving from a potential R, one uses the Lagrange equation [13, 15].

$$\begin{aligned}
\frac{da}{dt} &= \frac{1}{n^2 a}\frac{\partial R}{\partial \tau}\\
\frac{d\rho}{dt} &= \frac{1-\rho^2}{n^2a^2}\frac{\partial R}{\partial \tau} - \frac{\sqrt{1-\rho^2}}{na^2\rho}\frac{\partial R}{\partial \omega}\\
\frac{di}{dt} &= \frac{cotan(i)}{na^2\sqrt{1-\rho^2}}\frac{\partial R}{\partial \omega} - \frac{1}{na^2 sin(i)\sqrt{1-\rho^2}}\frac{\partial R}{\partial \Omega}\\
\frac{d\Omega}{dt} &= \frac{1}{na^2 sin(i)\sqrt{1-\rho^2}}\frac{\partial R}{\partial i}\\
\frac{d\omega}{dt} &= \frac{\sqrt{1-\rho^2}}{na^2\rho}\frac{\partial R}{\partial \rho} - \frac{cotan(i)}{na^2\sqrt{1-\rho^2}}\frac{\partial R}{\partial i}\\
\frac{d\tau}{dt} &= \frac{2}{n^2 a}\frac{\partial R}{\partial a} + \frac{1-\rho^2}{n^2a^2\rho}\frac{\partial R}{\partial \rho}
\end{aligned} \tag{2}$$

where i is the angle of inclination , Ω is the longitude of the ascending node, ω is the angle of the perigee and τ is the time of the perigee passage.

Alternatively a set of symplectic variables called Delaunay variables and related to the orbital elements can be introduced

$$\begin{array}{lll} L=\sqrt{a}, & G=\sqrt{a(1-\rho^2)}, & H=cos(i)\sqrt{a(1-\rho^2)},\\ l=M, & g=\omega, & h=\Omega \end{array}$$

where M is the mean anomaly.

The effect of the J_2-effect and lunar perturbation on the satellite motions are well understood and we use the computations excerpted from [12]. They are related to solar perturbation of the Moon. In this reference, they study Moon motion under the Sun perturbation, which we can adapt to the Earth-Moon-satellite case.

3.2. The J_2-effect

The Earth is modelled by an homogeneous oblate ellipsoid of revolution whose axe of symmetry is identified to the axis of rotation passing through the pole denoted Oz and the position of the satellite can be represented in spherical coordinates (r, λ, ϕ), λ being the latitude and ϕ the longitude.

The perturbing potential in the normalized coordinates takes the form [12]

$$R_1 = \frac{1}{2r}\left(\frac{R_e}{r}\right)^2 J_2(1-3sin^2(\phi))$$

where we have the relation

$$sin(\phi) = sin(i)sin(\omega+v)$$

where v is the true anomaly. Hence the perturbing potential is given by

$$R_1 = \frac{3}{2}\frac{R_e^2 J_2}{a^3}\left(\frac{a}{r}\right)^3\left[\frac{1}{3} - \frac{1}{2}sin^2(i) + \frac{1}{2}sin^2(i)cos(2(\omega+v))\right]. \tag{3}$$

The averaged perturbation computed by the formula

$$\overline{R_1} = \frac{1}{2\pi}\int_0^{2\pi} R dM$$

where M is the mean anomaly gives the following.

Proposition 3.3. *The averaged perturbation associated to the J_2-effect is described by the potential*

$$\overline{R_1} = \frac{3}{2}\frac{R_e^2 J_2}{a^3(1-\rho^2)^{\frac{3}{2}}}\left(\frac{1}{3} - \frac{1}{2}sin^2(i)\right).$$

3.3. The lunar perturbation

In the case of lunar perturbation, the perturbation depends upon two angular variables, the longitude l of the satellite and the longitude l' of the Moon. In order to have a rough evaluation of the perturbation we use a simplified model in [12] based on the following assumptions : the eccentricity of the satellite ρ is small and the inclination i of the Moon with respect to the Earth-satellite plane is small. The perturbing potential is described in [12, p.120] and the averaging process leads to the averaged potential

$$\overline{R_2} = \frac{n'^2 a^2}{4}\left(1 + \frac{3}{2}\rho^2 - \frac{3}{2}i^2\right) \tag{4}$$

where n' is the normalized mean movement of the Moon which corresponds to the scaling parameter of the lunar perturbation (see [6] for a more general case).

3.4. Superpostion of the perturbations

The two perturbations have to be represented with respect to a similar reference plane. Concerning the J_2-effect the reference plane with zero inclination is the equatorial plane, while for the lunar perturbation, the reference plane is the Earth-satellite plane.

A simplified academic model is to take both the inclination to zero and restrict the control to this plane. In this case, one can restrict the metric to the 3D-Riemannian metric described by $\overline{H_1}$ whose properties are completely described in [2]. Note that for this representation to be coherent $sin(i)$ has to be approximated by i in $\overline{R_1}$ expression. Also in this model, we neglect the difference between averaging with respect to the longitude and the mean anomaly.

4. Computations

4.1. Shooting equation

Let $\vec{H}$ be an Hamiltonian vector field associated to the Zermelo navigation problem, $z = (x, p)$, $x \in \mathcal{X}$, denoting the state and adjoint vector and H

being homogeneous of degree 1 in p. Fixing the initial and final state vectors (x_0, x_1) and t_F being the transfer time the shooting equation is defined by

$$S : p_0 \mapsto \Pi(exp(t_F \vec{H}(z_0)) = x_1$$

where $z_0 = (x_0, p_0)$, $\Pi : (x, p) \mapsto x$ and p_0 can be normalized by homogeneity.

4.2. The geometric concept of conjugate point

Definition 4.1. Let $z = (x, p)$ be a reference extremal solution of $\vec{H}$ on $[0, t_F]$. The variational equation

$$\dot{\delta z}(t) = d\vec{H}(z(t))\delta z(t)$$

is called the Jacobi equation. A Jacobi field is a non trivial solution $\delta z = (\delta x, \delta p)$ of Jacobi equation and it is said to be vertical at time t if $\delta x(t) = 0$.

Definition 4.2. We define the exponential mapping

$$exp_{x_0,t}(p_0) = \Pi(z(t, x_0, p_0))$$

where p_0 can be restricted to the sphere $|p_0| = 1$. If $z = (x, p)$ is the reference extremal, a time $t_c > 0$ is said to be conjugate to 0 if the mapping $p_0 \mapsto exp_{x_0,t}(p_0)$ is not of rank $n-1$ at $t = t_c$ (with $n = dim\mathcal{X}$) and the associated point $x(t_c)$ is said to be conjugate to x_0. We denote by t_{1c} the first conjugate time and $C(x_0)$ is the conjugate locus formed by the set of first conjugate points.

Testing conjugary. An algorithm can be deduced which is implemented in the Hampath Code [5] used in our numerical simulations. Let $z(t) = (x(t), p(t))$ be the reference extremal and consider the vector space of dimension $n-1$ generated by the Jacobi fields $\delta z_i = (\delta x_i, \delta p_i), i = 1, ..., n-1$ vertical at $t = 0$ and such that $\delta p_i(0)$ is orthogonal to p_0. At a conjugate time t_c, one has

$$rank[\delta x_1(t_c), ..., \delta x_{n-1}(t_c)] < n - 1$$

or equivalently,

$$det[\delta x_1(t_c), ..., \delta x_{n-1}(t_c), \dot{x}(t_c)] = 0.$$

Hampath Code. This code is used to

- Integrate the Hamiltonian flow and compute the Jacobi fields along a given solution.
- Solve the shooting equation.

4.3. Computations

Our working example is associated to the model introduced in section 3.3 where the averaged perturbation is given by

$$\overline{P} = \underbrace{\lambda_1 \frac{n^2}{(1-\rho^2)^{\frac{3}{2}}}}_{J_2\ effect} + \underbrace{\lambda_2 \frac{n'^2}{4n^{\frac{4}{3}}}(1 + \frac{3}{2}\rho^2)}_{lunar-perturbation} \tag{5}$$

where λ_1, λ_2 are scaling parameters.

Using $n = a^{-\frac{3}{2}}$, ρ and θ as coordinates the Lagrange equations (2) give the averaged vector field

$$\begin{aligned}\frac{d\overline{n}}{dt} &= \frac{d\overline{\rho}}{dt} = 0\\ \frac{d\overline{\theta}}{dt} &= \frac{n^{\frac{1}{3}}\sqrt{1-\rho^2}}{\rho}\left[\frac{3\lambda_1 n^2\rho}{(1-\rho^2)^{\frac{5}{2}}} + \frac{3\lambda_2\rho}{n^{\frac{4}{3}}}\right]\\ &= \frac{3\lambda_1 n^{\frac{7}{3}}}{(1-\rho^2)^2} + \frac{3\lambda_2\sqrt{1-\rho^2}}{n}.\end{aligned}$$

This leads to the averaged Hamiltonian

$$\begin{aligned}\overline{H} =& p_\theta\left[\frac{3\lambda_1 n^{\frac{7}{3}}}{(1-\rho^2)^2} + \frac{3\lambda_2\sqrt{1-\rho^2}}{n}\right]\\ &+ \lambda\sqrt{\frac{1}{4n^{\frac{5}{3}}}\left[18n^2p_n^2 + 5(1-\rho^2)p_\rho^2 + (5-4\rho^2)\frac{p_\theta^2}{\rho^2}\right]}\end{aligned} \tag{6}$$

where λ is the scaling parameter of the control maximal magnitude.

4.4. Numerical results

This section is achieved by a series of numerical computations on the free system, on extremal trajectories and on conjugate loci. This is an academic application where the satellite and the Moon belong to the equatorial plane. The J_2-effect is not taken into consideration. The simulations are computed thanks to the Hampath code [5].

Free system. The control is set to zero and the dynamical system is deduced from the Lagrange equations and the perturbative potential (5). The solutions are expressed in the $(n(t), \psi(t), \theta(t))$ coordinates where ϕ is the angle such that $\rho = sin(\phi)$, and $\psi(t) = \frac{\pi}{2} - \phi(t)$.
Figures 1 and 2 yield two first integrals of the double averaged Hamiltonian system. The double average is taken with respect to the mean motion variables M and M' which correspond respectively to the satellite and the Moon. This integral over $(M, M') \in [0, 2\pi] \times [0, 2\pi]$ is computed with M' fixed with respect to M and the slow variables.
The variation of $\overline{\theta}(t)$ is equal to $\frac{3}{4}\frac{n'^2}{\overline{n}}(1 - \frac{\overline{\rho}^2}{2}) \approx 2.8\,^\circ$ during one lunar revolution around the Earth.
Controlled system. Due to the homogeneity of order 1 of the Hamiltonian (6), the time-minimum problem is considered and the adjoint vector is normalized. Extremal trajectories are computed for different values of λ. The shooting algorithm is performed to solve the boundary value problem by determining the initial adjoint vector $p(0)$ and the optimal time t_f.
In the following figures, the perturbed case ($\lambda = 10^{-1}$) is represented in solid line and is compared to the unperturbed case represented in dash-dot line. The final points are indicated by cross markers. The first conjugate points, indicated by star markers, are computed thanks to the algorithm presented

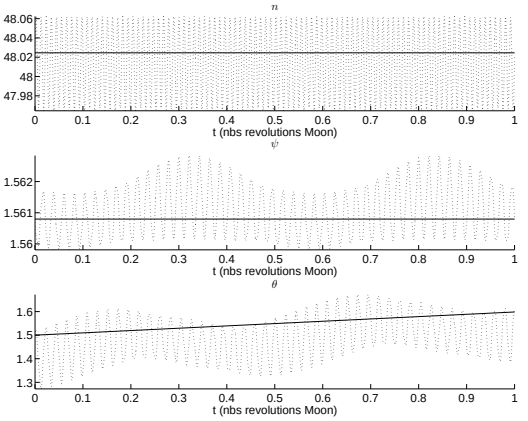

FIGURE 1. Evolution of n, ψ and θ of the double averaged (dotted line) and the non averaged (solid line) free system over one lunar revolution around the Earth.

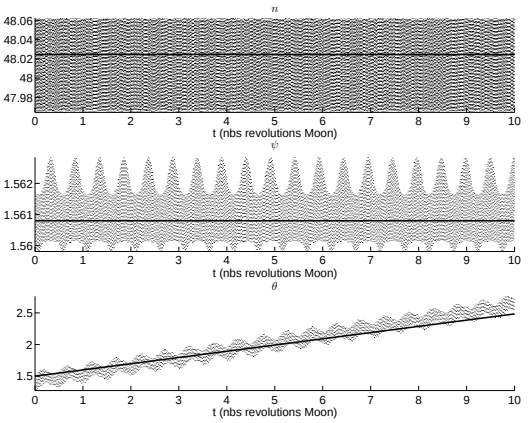

FIGURE 2. Evolution of n, ψ and θ of the double averaged (dotted line) and the non averaged (solid line) free system over ten lunar revolutions around the Earth.

in the subsection 4.2 for which the time evolution of the determinant of the matrix $(\delta x_1(t)\ \delta x_2(t)\ \dot{x}(t))$ is presented in Figure 8.

Figures 9 and 10 represent the projection of the extremal trajectories in (ψ, θ) coordinates starting from the initial point $(\rho_0, \theta_0) = (0.60, \pi)$ in the unperturbed and perturbed case.

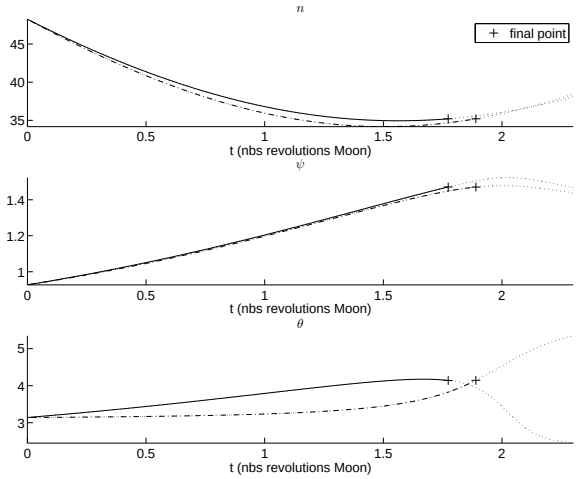

FIGURE 3. Evolution of state vectors of extremal trajectories from the initial state point $(n_0, \rho_0, \theta_0) = (48.3, 0.60, \pi)$ to the final state point $(n_f, \rho_f, \theta_f) = (35.2, 0.10, \pi + 1)$. The comparison is performed between the perturbed case (solid line) and the unperturbed one (dash-dot line). Final points are indicated (cross markers).

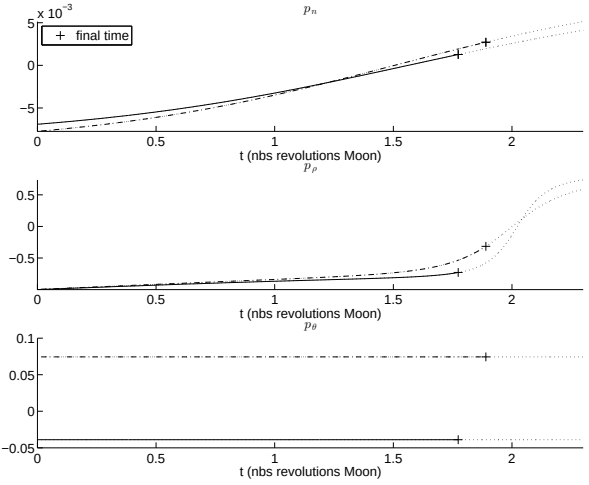

FIGURE 4. Evolution of adjoint vectors of extremal trajectories from the initial state point $(n_0, \rho_0, \theta_0) = (48.3, 0.60, \pi)$ to the final state point $(n_f, \rho_f, \theta_f) = (35.2, 0.10, \pi+1)$. Final points are indicated.

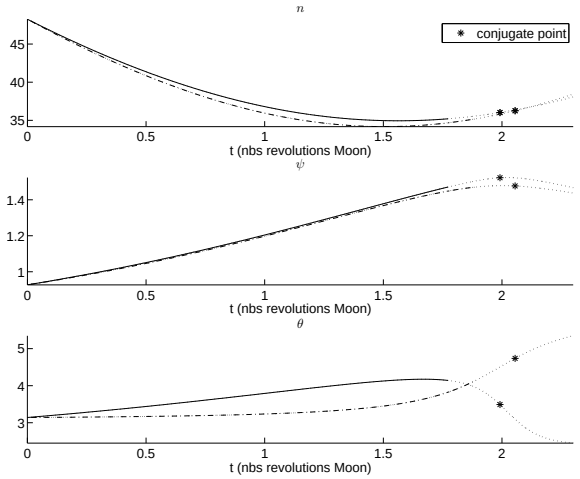

FIGURE 5. Evolution of state vectors of extremal trajectories from the initial state point $(n_0, \rho_0, \theta_0) = (48.3, 0.60, \pi)$ to $(n_f, \rho_f, \theta_f) = (35.2, 0.10, \pi + 1)$. Conjugate points are indicated (star markers).

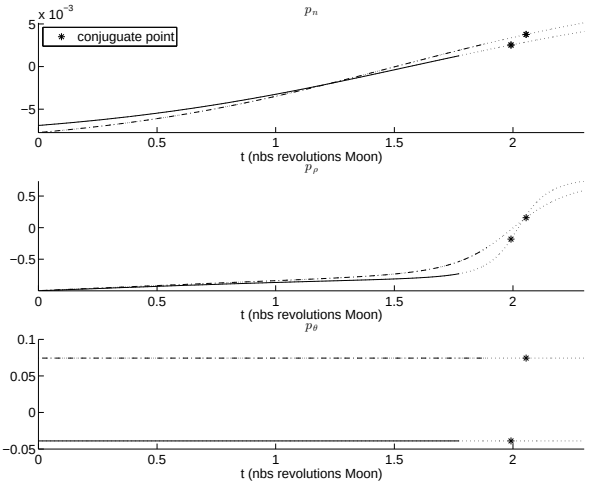

FIGURE 6. Evolution of adjoint vectors of extremal trajectories from the initial state point $(n_0, \rho_0, \theta_0) = (48.3, 0.60, \pi)$ to the final state point $(n_f, \rho_f, \theta_f) = (35.2, 0.10, \pi + 1)$. Conjugate points are indicated.

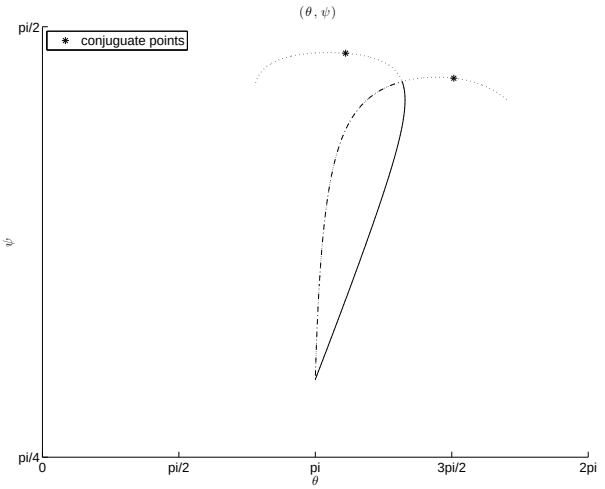

FIGURE 7. Projection of extremal trajectories in (ψ, θ) coordinates in the perturbed case (solid line) and the unperturbed one (dash-dot line).

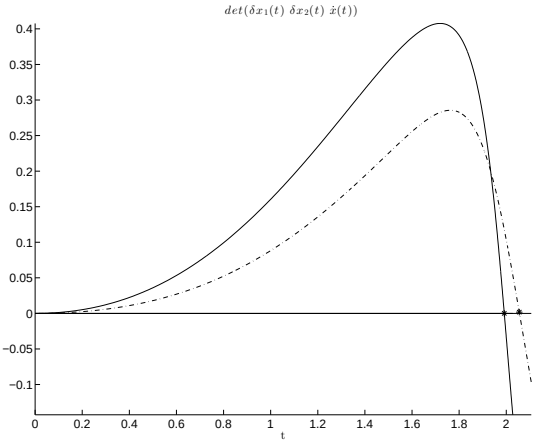

FIGURE 8. Rank condition for the determination of the first conjugate point for the perturbed case and the unpertubed one. The first zero of the determinant is the first conjugate time.

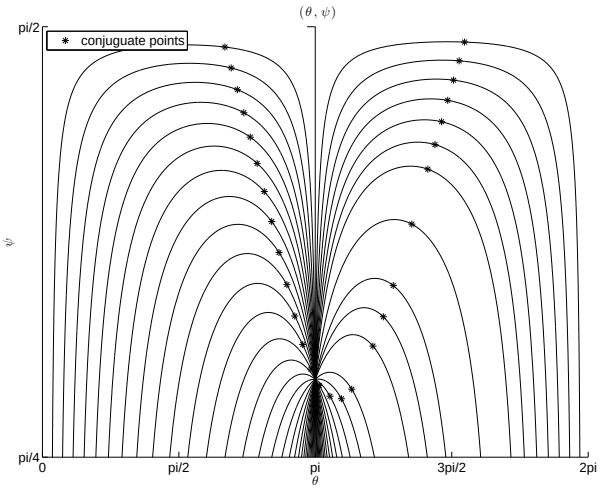

FIGURE 9. Projection of extremal trajectories in the unperturbed case in (ψ, θ) coordinates starting from the same initial point $(\rho_0, \theta_0) = (0.60, \pi)$. Conjugate points are indicated.

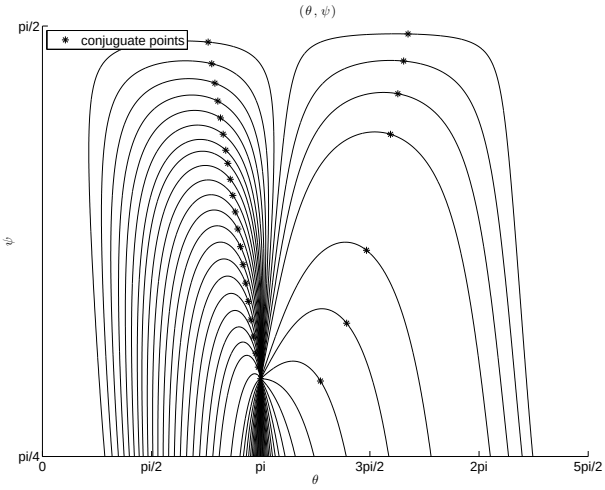

FIGURE 10. Projection of extremal trajectories in the perturbed case ($\lambda = 1$) in (ψ, θ) coordinates starting from the same initial point $(\rho_0, \theta_0) = (0.60, \pi)$. Conjugate points are indicated.

References

[1] B. Bonnard and J.-B. Caillau. Riemannian metric of the averaged energy minimization problem in orbital transfer with low thrust. *Ann. Inst. H. Poincaré Anal. Non Linéaire*, 24(3):395–411, 2007.

[2] B. Bonnard and J.-B. Caillau. Geodesic flow of the averaged controlled Kepler equation. *Forum Math.*, 21(5):797–814, 2009.

[3] Arthur E. Bryson, Jr. and Yu Chi Ho. *Applied optimal control*. Hemisphere Publishing Corp. Washington, D. C.; distributed by Halsted Press [John Wiley & Sons], New York-London-Sydney, 1975. Optimization, estimation, and control, Revised printing.

[4] C. Carathéodory. *Calculus of variations and partial differential equations of the first order. Part I: Partial differential equations of the first order*. Translated by Robert B. Dean and Julius J. Brandstatter. Holden-Day, Inc., San Francisco-London-Amsterdam, 1965.

[5] O. Cots. *Contrôle optimal géométrique: méthodes homotopiques et applications*. PhD thesis, Université de Bourgogne, 2012.

[6] RC Domingos, R Vilhena de Moraes, and AF De Almeida Prado. Third-body perturbation in the case of elliptic orbits for the disturbing body. *Mathematical Problems in Engineering*, 2008, 2008.

[7] Theodore N. Edelbaum. Optimum low-thrust rendezvous and station keeping. *AIAA J.*, 2:1196–1201, 1964.

[8] Theodore N. Edelbaum. Optimum power-limited orbit transfer in strong gravity fields. *AIAA J.*, 3:921–925, 1965.

[9] S. Geffroy. *Généralisation des techniques de moyennation en contrôle optimal, application aux problèmes de rendez-vous orbitaux à poussée faible*. PhD thesis, CNES, 1997.

[10] S. Geffroy and R. Epenoy. Optimal low-thrust transfers with constraints—generalization of averaging techniques. *Acta Astronautica*, 41(3):133–149, 1997.

[11] V. V. Nemytskii and V. V. Stepanov. *Qualitative theory of differential equations*. Princeton Mathematical Series, No. 22. Princeton University Press, Princeton, N.J., 1960.

[12] G. Pascoli. Eléments de mécanique céleste. *Eléments de mécanique céleste., by Pascoli, G.. Colin, Paris (France), 1993, 198 p., ISBN 2-200-21350-6, Price FF 135.00.*, 1, 1993.

[13] H. Poincaré. *Œuvres. Tome VII*. Les Grands Classiques Gauthier-Villars. [Gauthier-Villars Great Classics]. Éditions Jacques Gabay, Sceaux, 1996. Masses fluides en rotation. Principes de mécanique analytique. Problème des trois corps. [Rotating fluid masses. Principles of analytic mechanics. Three-body problem], With a preface by Jacques Lévy, Reprint of the 1952 edition.

[14] L. S. Pontryagin, V. G. Boltyanskii, R. V. Gamkrelidze, and E. F. Mishchenko. *The mathematical theory of optimal processes*. Translated from the Russian by K. N. Trirogoff; edited by L. W. Neustadt. Interscience Publishers John Wiley & Sons, Inc. New York-London, 1962.

[15] O. Zarrouati. Trajectoires spatiales. *Trajectoires spatiales.. O. Zarrouati. Cepadues-Editions, 111 rue Nicholas-Vauquelin, F-31100 Toulouse, France. 522 pp. Price FF 199.00 (1987). ISBN 2-85428-166-7.*, 1, 1987.

Bernard Bonnard
Institut de Mathématiques de Bourgogne
e-mail: bernard.bonnard@u-bourgogne.fr

Helen Henninger
INRIA
e-mail: helen.henninger@inria.fr

Jérémy Rouot
INRIA
e-mail: jeremy.rouot@inria.fr